

# Effect of surface preparation on corrosion of steel rebars coated with cement-polymer-composites (CPC) and embedded in concrete

Deepak K. Kamde, Radhakrishna G. Pillai \*

Department of Civil Engineering, Indian Institute of Technology Madras, Chennai, India

## HIGHLIGHTS

- First paper on performance of CPC coated steel rebars considering the possible quality issues at construction sites.
- Paper covers from microstructure aspects of corrosion to the service life of a bridge structure.
- Possible corrosion mechanism for inadequately applied CPC coated steel is proposed.
- When CPC coatings are used, sandblasting of steel rebar can enhance the service life by twice.

## ARTICLE INFO

### Article history:

Received 19 June 2019

Received in revised form 11 November 2019

Accepted 12 November 2019

Available online 26 November 2019

### Keywords:

Reinforced concrete

Surface preparation

Chloride threshold

Cement polymer composite coating

Time to corrosion initiation

## ABSTRACT

Nowadays, Cement-Polymer-Composites are widely used to coat steel rebars to delay the initiation of corrosion in reinforced concrete (RC) structures. However, Cement-Polymer-Composite (CPC) coating is sometimes inadequately applied on rusted steel and can lead to premature under film/crevice corrosion. This paper investigates the effect of such inadequate applications of CPC coating and premature corrosion on the service life of RC structures. For this, maximum surface chloride concentrations, diffusion coefficients, and chloride thresholds were determined by a one-year-long laboratory study on the specimens obtained from a 6-year-old bridge and prepared in the laboratory. Studies found that the chloride threshold of inadequately coated steel rebar (i.e., coating on 'as received' surface) is significantly lower than that of the adequately coated steel rebars (i.e., coating on 'sandblasted' surface). Also, the corrosion initiation time for systems with inadequately coated steel rebar was about 50% less than that of the systems with adequately coated steel rebars. The corrosion mechanisms were justified with micrographs. It is recommended not to use CPC coated steel rebars if adequate surface preparation (say, cleaning/sandblasting) is not implemented.

© 2019 Elsevier Ltd. All rights reserved.

## 1. Introduction

In the past two decades, a lot of reinforced concrete (RC) structures, such as highway/railway bridges, high-rise buildings, and power plants, have been constructed with a target service life of

more than 100 years. Many of these RC structures are exposed to highly aggressive environments. To achieve this desired long life, the steel-cementitious (SC) systems in these structures must have good corrosion resistance. Generally, the steel reinforcing bars ('rebars', herein) are coated with organic materials to enhance their corrosion resistance. Usually, these coatings are made of either a polymer or a polymer-modified material. In general, these types of organic coatings work by (i) providing a shield/physical barrier between the underlying steel and the deleterious elements, such as moisture, oxygen, chlorides, and (ii) restricting the ionic flow between anodic and cathodic areas [1–3,4]. The polymer-modified cementitious coatings have an additional feature of forming a complex protective film by reacting with the metal surface. This protective film can enhance the corrosion resistance of steel coated with cementitious coatings. The cement-polymer-composite (CPC) with acrylic base is a type of organic coating that

*Abbreviations:* %bwob, % by weight of binder; AR, As-received;  $C(x, t)$ , Chloride concentration at depth 'x' after exposure for 't' seconds; CDF, Cumulative distribution function;  $C_{max}$ , Maximum chloride concentration at the exposed concrete surface; CPC, Cement-Polymer-Composite;  $C_s$ , Surface chloride concentration;  $Cl_{th}$ , Critical chloride threshold of steel-concrete interface;  $D_{cl}$ , Diffusion coefficient of concrete; *erf*, Error function; *m*, Decay constant; RC, Reinforced Concrete; SB, Sandblasted; SC, Steel-Cementitious; *t*, Exposure time;  $t_i$ , Time to corrosion initiation; wC, With coating; woC, Without coating; *x*, Depth from the exposed surface of concrete.

\* Corresponding author.

E-mail address: [pillai@iitm.ac.in](mailto:pillai@iitm.ac.in) (R.G. Pillai).

is widely used in the construction industry. The CPC coating is supposed to be applied onto sand-blasted (SB) rebars at sites. Literature provides sufficient information on the corrosion resistance of SB/clean rebars with CPC and other organic coatings modified with cement/fly ash [4–8]. However, it should be noted that many site personnel may not insist on sandblasting or cleaning the rebars prior to applying the CPC coating; and use rebars with as-received (AR) conditions. The as-received steel may have the possible presence of rust on the rebar surface leading to premature corrosion.

NACE impact report states that nearly 50% of structures experience a major repair within 10 years [9]. The costs of corrosion for some developing and developed nations were estimated to be about 3–4% of GDP [9,10]. If the practices of coating onto inadequately cleaned rebars continue, then it may lead to premature corrosion – leading to reduced service life and higher cost of corrosion.

The remaining paper is organized in the following manner. First, a review of corrosion mechanisms and performance of organic coatings in chloride environment is discussed. Then, a brief introduction about CPC coating, followed by the problem statement is provided. Further, field investigation and experimental program to determine the maximum surface chloride concentration, diffusion coefficient, and chloride threshold are discussed. Using these input parameters, the time to corrosion initiation of RC structural elements is estimated and compared. The proposed corrosion mechanisms are then justified using the scanning electron micrographs. Later, remedial measures to delay the corrosion initiation are suggested. Finally, conclusions drawn from this research are provided.

### 1.1. Corrosion performance of organic coatings in various applications

In the automobile and oil/gas sectors, coatings are applied by skilled workers and only on clean metallic surfaces in a dust-free environment with controlled temperature. In such conditions, coating materials get adhered well to the metal surface and prevent the premature, under film corrosion [8]. On the other hand, in the civil construction sector, cementitious coatings to steel reinforcement are often applied by unskilled workers at construction sites. This can lead to various issues associated with poor steel surface preparation and application of coating materials.

At present, many organic coatings are commercially available with the following resin as base material: epoxy, acrylic, polyester, etc. If pure organic coatings (i.e., without any additives) are used, then moisture and oxygen can easily penetrate through the coating and result in crevice corrosion and/or under-film corrosion [11–14]. However, when additives, such as cement, fly ash, nano-clay, and composites of these materials, are mixed with epoxy/acrylic resins, they can disperse uniformly into small platelets. These small platelets can result in denser microstructure of the coatings [15]. Therefore, with the inclusion of additives, the absorption/penetration of water and oxygen can be significantly reduced [16,17]. Further, the shape, size, and pH of additives can also influence the migration, inhibition (under-film corrosion or re-passivation), and workability of the coating material. For example, flaky or small-sized additives can provide a tortuous path for corrosion species to travel and offer higher resistance to the penetration of corrosive species [18]. Therefore, if cement/fly ash (particle size of about 1–100  $\mu\text{m}$ ) is used as an additive, they can act as a filler and delay the diffusion of corrosive species through the coating [15,19]. They also help in the formation of a strong passive film by providing an alkaline environment to the steel surface [20,21]. Therefore, this can increase the resistance against the under-film corrosion [7]. In addition, the spherical shape of fly ash can enhance the workability of coating and make it easy to apply on rebars [15]. All these prop-

erties can be achieved only if the steel surface is sandblasted/cleaned adequately. Achieving this is a challenge in the civil construction industry – mainly due to the large-scale usage of rebars and poor workmanship. Literature report on the improved corrosion performance of steel when coated with organic coatings; however, these studies are carried out on cleaned steel surface [4–8,21], which is not the usual practice at construction sites. Significant concern exists on the corrosion performance of coated steel reinforcement with the presence of rust beneath the coating [18]. Such issues and their impact on the service life of concrete structures are the focus of this paper.

### 1.2. Corrosion performance of organic coatings used in construction applications

Organic coatings are widely used to coat the reinforcing steel to delay the onset of corrosion by restricting the transport of moisture and chlorides to the steel surface. Fusion-Bonded-Epoxy (FBE) coated rebar is one of the most widely used coated rebars in the construction industry [22,23]. Much literature is available on corrosion performance of Fusion-Bonded-Epoxy (FBE) coated steel rebars. Some of the literature shows that the FBE coated steel performs well in chloride contaminated environment [2,3,24]. However, some literature reports that the structures with FBE coated steel experienced initiation of corrosion within 30 years of service life [11,14,25]. In a few of these cases, the coating was damaged by bending and dragging of the coated rebars, and also exposed to sunlight during the storage at construction sites [26]. Damage to coating can result in moisture-induced corrosion without sufficient chloride at the rebar level [27]. Therefore, studies on the chloride threshold of these rebars are not available.

On the other hand, cement-based polymer coatings provide an alkaline environment to the steel surface [2]. This may form a stable passive layer on the steel surface. Therefore, high chloride concentration (chloride threshold) may be required to initiate the corrosion activity. But, literature on the chloride threshold of steels coated with cement-based organic coatings is not available. Note that a few literature focuses on evaluating the performance of organic coating by using various test methods, such as flexibility test, impact resistance test, salt spray test, and quantification of charge transfer resistance [21], where four out of 16 coatings could not meet the requirements for selection of organic coatings (see Table 1). Please note that these test methods will not help in true estimation of their performance and the service life of RC structures. Therefore, a study on the determination of chloride threshold of coated steel with cementitious coatings is essential to quantify the service life of RC structures with coated steel, especially when it is applied inadequately on steel surfaces.

The CPC coating consists of two coats (a rapid setting primer coat followed by a cement polymer sealant coat). Both the primer and sealant contain thermoplastic acrylic resins. In addition, sealant is mixed with cement powder as an additive. The CPC coating is supposed to be applied on the steel surface after sandblasting/cleaning. Sandblasting can remove the rust, dirt, oil, etc., which could be contaminated by chlorides. Sandblasting results in the large surface area of steel for chemo-mechanical bonding between the bare steel and coating material [28]. It may be noted that the cementitious components in the CPC coating can react with the steel surface and form a stable passive layer of oxides. Fig. 1 shows an example of inadequately applied CPC coating on the rebar of a bridge pier of a coastal highway. The photograph was taken during the construction time and it is evident that the coating is not applied to the top regions of the vertical rebars. Also, the close-up image shows the incomplete application of CPC coating, especially at the rebar intersections. These indicate that the coating is applied at the site after the rebars are tied in position, and on

**Table 1**  
Corrosion performance of various organic coatings [21].

#	Resin							Pigment				Ranking for each test			
	AP	AI	PP	AcR	Ep	Si	PA	TiO <sub>2</sub>	Zn <sub>3</sub> (PO <sub>4</sub> ) <sub>2</sub>	OPC	FA	FT	IRT	SS	CTR
1	✓	✓						✓	✓	✓		1	1	2	Pass
2	✓	✓						✓	✓		✓	1	1	5	Fail
3	✓	✓							✓	✓		1	1	7	Fail
4	✓	✓							✓		✓	1	1	8	Fail
5		✓	✓						✓	✓	✓	1	1	6	Pass
6		✓	✓					✓	✓		✓	1	1	3	Pass
7		✓	✓						✓	✓		1	1	4	Fail
8		✓	✓						✓		✓	1	1	1	Fail
9				✓					✓	✓	✓	2	1	7	Fail
10				✓				✓	✓		✓	1	1	7	Fail
11				✓					✓	✓		2	1	3	Fail
12				✓					✓		✓	1	1	3	Fail
13					✓	✓	✓		✓	✓	✓	1	1	6	Fail
14					✓	✓	✓	✓	✓		✓	1	1	2	Pass
15					✓	✓	✓		✓	✓		1	1	2	Fail
16					✓	✓	✓		✓		✓	1	1	2	Fail

AI, Aromatic isocyanate; AcR, Acralic resin; AP, Acrylic polymer; CTR, Charge transfer resistance; Ep, Epoxy; FA, Flyash; FT, Flexibility test; IRT, Impact resistance test; OPC, Ordinary Portland Cement; PA, Polyamide; PP, Polyester polyli; Si, Silicon; SS, Salt spray test.

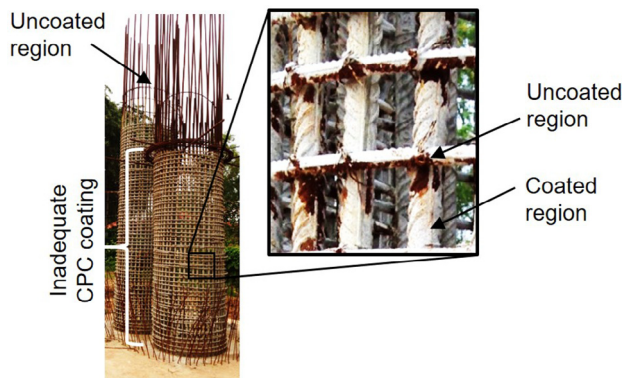


**Fig. 1.** Photograph of a column under construction with CPC coated rebars and close-up showing inadequate CPC coating on rebars.

'as-received' steel surfaces with rust. The application of the coating on the as-received steel surface can result in inadequate chemo-mechanical bonding and passive film – resulting in premature and/or under film corrosion. The use of coating on as-received rebars could lead to a much lower chloride threshold and service life than the case with coating on SB rebars; however, many site personnel wrongly believe that the CPC coating could perform even without steel surface cleaning. Therefore, the focus of this paper is to quantify these differences in chloride threshold due to the difference in the surface conditions of the CPC coated steel rebars and their effect on service life.

Though CPC coating (or cement-based polymer modified coating) is widely used in India. Many cement/fly ash based polymer modified coatings are being used in different parts of the world. For example, Pei et al. (2015) and Pei et al. (2017) compared the bond and corrosion performance of six combinations of cementitious capillary crystalline waterproofing coating (CCCW), which is widely used in Canada [29,30]. Likewise, Jorge et al. (2012) compared the bond between steel rebars coated with cement-based anticorrosive coatings, and repair mortar [31]. These coating materials are used for concrete repair in some parts of Europe. In addition, Tang et al. (2012) reported the corrosion performance of cement-modified enamel coatings, showing the use of cement-based coatings in USA [6]. Likewise, Wang et al. (2014) compared the corrosion performance of polymer-modified cement-based coatings perform superior to FBE coated steel, showing the use of

such coated rebar is ongoing in China as well [32]. The use of organic coatings modified with cementitious additive is a worldwide practice. Therefore, understanding the corrosion mechanisms of coated steels with cement-based organic coatings will help to overcome the quality issues related to coating application practices.

## 2. Research significance

Recently, many developing countries are witnessing construction boom. Unfortunately, many constructions are happening with poor quality materials and poor applications due to the race for fast-track construction and low quest for quality/durability among some of the stakeholders. One such example is the use of steel rebars with the inadequate application of cement polymer composite (CPC) coating material. This paper provides the field and laboratory data indicating that the use of inadequately coated steel rebars (coating on as-received rebars) can lead to at least 40% lower service life than the adequately coated systems (coating on sand-blasted rebars). If the use of poorly coated rebars continues, then many large scale infrastructure systems will incur the high cost of corrosion. This paper will help engineers to quantitatively estimate the effect of poorly coated rebars on the service life of reinforced concrete structures and develop strategies to ensure the use of quality materials and construction/maintenance practices.

## 3. Field inspection and experimental program

A 6-year old concrete bridge located in the chloride-rich environment (within 2 km from the sea) of a coastal city in India was considered for this study. Fig. 2 (a) shows the schematic showing the girder, pier, pile cap, and pile of this bridge. The bridge experiences around 4 months of heavy rain in a year and the ambient relative humidity ranges between 70 and 85% during the rest of the year. Therefore, sufficient moisture is expected to be always available at the surface of the embedded rebar. This makes it a favourable condition for the chloride-induced corrosion process [33]. The desired service life of the bridge is 120 years. To achieve this long life, the CPC coated steel rebars were proposed by designers. However, CPC coating was applied on 'as-received' steel surface. (instead of 'sand-blasted' steel surface). This practice can lead to poor corrosion resistance. Cementitious binders with 25–30%

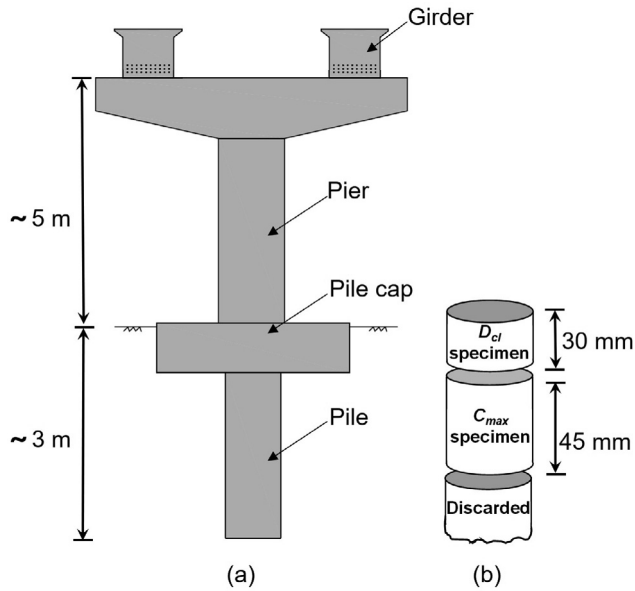


**Fig. 2.** Schematics of (a) bridge elements under study and (b) cylindrical concrete specimens cored from the bridge elements [Not drawn to scale].

**Table 2**  
Details of the concrete mix used in the bridge.

Ingredient	Pile cap and pile (M35), kg	Pier (M45), kg	Girder (M60), kg
Cement (C)	280	390	440
Fly ash (F)	130	145	125
20 mm aggregate	438	0	500
12.5 mm aggregate	605	802	687
Manufactured Sand	737	953	640
Total water	223.6	215.9	183.0
(C + F): FA: CA	1:1.45:2.05	1:1.76:1.48	1:1.13:2.10
Admixture (%bwob)	0.55	0.70	1.10
Retarder (%bwob)	0.10	0.20	0.10

Class – F fly ash was used in making the M60, M45, M35, and M35 grade concretes for the girders, piers, pile caps, and piles, respectively (see Table 2 for mix design).

The bridge being located in a coastal city, the governing deterioration mechanism could be chloride-induced corrosion. As a conservative practice, service life can be considered as the time to corrosion initiation,  $t_i$ , which is defined as the time taken by the chlorides to travel through the cover concrete to reach the steel rebar, and initiate the active corrosion. The  $t_i$  can be estimated by using the (i) the maximum chloride concentration at the concrete surface ( $C_{max}$ ), (ii) the chloride diffusion coefficient of cover concrete ( $D_{cl}$ ), and (iii) the critical chloride threshold of the steel-concrete interface ( $Cl_{th}$ ) and the Fick's 2<sup>nd</sup> law of diffusion. To obtain  $C_{max}$  and  $D_{cl}$ , cylindrical concrete specimens of about 90 mm diameter and 100 mm length were extracted from the girder, pier, pile cap, and pile elements and laboratory experiments were performed. To determine the  $Cl_{th}$ , the as-received and sandblasted rebars were collected from the bridge site. Then, the CPC coating was applied, and experiments were performed in the laboratory. In this, the effect of surface preparation on the  $Cl_{th}$  of rebars was studied. Details on the experimental programs adopted to determine these parameters are discussed below.

### 3.1. Maximum chloride concentration at the exposed concrete surface ( $C_{max}$ )

$C_{max}$  is the maximum chloride concentration that can get accumulated on the exposed surface of the concrete. The  $C_{max}$  depends

on water-to-binder ratio (w/b), the percentage of fly ash in the cementitious binder, cement content, and the ambient chloride concentration [34]. Many literature report that surface chloride concentration increases with the exposure time [35–37]. Therefore,  $C_{max}$  can be determined by long-term exposure (say, several years) of the concrete specimen to the chloride-rich environment. However, such long exposure may not be always possible. Nemecek et al. (2018) and Devi (2012) reported that accelerated testing underestimates the  $C_{max}$ , leading to the overestimation of service life [38,39]. The aim of this study is to compare the service life of various elements of the bridge with different steel surface conditions. Therefore, rapid migration tests (i.e., NT-build 492) were conducted on concrete specimens extracted from the bridge [40]. It was experimentally found that the chloride concentration was less than 0.02 %bwob at depths greater than 30 mm from the surface. Hence, a 45 mm thick slice was cut from the extracted cylindrical core specimen for  $C_{max}$  study, as shown in Fig. 2 (b). The experimental test setup used for migration test was the same as that described in NT-build 492. After the completion of the migration test, the average chloride concentration of the 5 mm thick concrete layer in contact with the chloride solution (during the migration test) was determined and defined as  $C_{max}$ . Later, this  $C_{max}$  was used to determine the time to corrosion initiation.

### 3.2. Chloride diffusion coefficient of concrete ( $D_{cl}$ )

Fig. 2(b) shows the 30 mm thick test specimen sliced from the extracted core and used to determine  $D_{cl}$ . As per ASTM C1556 (2015), chloride profiles up to 25 mm were obtained for each specimen [41]. Lathe machine and single head diamond dresser tool were used for grinding these concrete specimens. The powdered samples from each layer were collected, and chloride concentrations were determined as per SHRP-S-330 (1993) [42]. Later, these chloride profiles and Fick's second law (Eq. (1)) were used to determine the  $D_{cl}$ .

$$C(x, t) = C_s - (C_s - C_i) \times \operatorname{erf}\left(\frac{x}{\sqrt{4 \times D_{cl} \times t}}\right) \quad (1)$$

where, ' $C(x, t)$ ' is the chloride concentration measured at depth ' $x$ ' from the exposed concrete surface at exposure time of ' $t$ ' seconds, ' $C_s$ ' is the surface chloride concentration built-up on the exposed concrete surface after exposure time of  $t$  seconds, ' $C_i$ ' is the initial chloride concentration (assumed to be zero in this study), ' $D_{cl}$ ' is apparent chloride diffusion coefficient, and ' $\operatorname{erf}()$ ' is the mathematical error function. Here,  $D_{cl}$  is considered as a time-variant function and determined by using Eq. (2),

$$D_{cl}(t) = D_{cl} \times \left(\frac{t_0}{t}\right)^m \quad (2)$$

where ' $D_{cl}(t)$ ' is the chloride diffusion coefficient at time  $t$ , ' $D_{cl}$ ' is chloride diffusion coefficient of concrete at the age of 28 days, ' $t$ ' is the age of the bridge in days, ' $t_0$ ' is age equal to 28 days, and ' $m$ ' is the decay constant, which was calculated using Eq. (3) [43].

$$m = 0.2 + 0.4 \left(\frac{FA(\text{in}\%)}{50}\right) \quad (3)$$

where ' $m$ ' is the decay constant (also known as ageing coefficient), which influences the rate of reduction of  $D_{cl}$  of concrete as a function of time. The term FA stands for the replacement level (in %) of fly ash in the concrete.

### 3.3. Chloride threshold of steel-coating-concrete interfaces ( $Cl_{th}$ )

Chloride threshold ( $Cl_{th}$ ) is the minimum chloride concentration required at the steel-coating-concrete interface to initiate active

corrosion. Table 3 shows the details of test variables and the number of specimens cast to evaluate the effect of steel surface preparation and CPC coating on the chloride threshold of steel rebars. Following steel surface and coating conditions were studied: (i) 'as-received' steel rebar without coating (AR-woC), (ii) 'as-received' steel rebar with coating (AR-wC), (iii) 'sand-blasted' steel rebar without coating (SB-woC), and (iv) 'sand-blasted' steel rebar with coating (SB-wC). Five macrocell corrosion specimens each with these four types of steel rebars were prepared (total 20 specimens) and exposed to chlorides until corrosion measurements confirm the initiation of corrosion.

### 3.3.1. Specimen preparation

To prepare the CPC coated steel, one thin layer of CPC primer was applied on the uncoated steel surfaces (AR and SB) and allowed to dry for a minimum of 30 min. To avoid the discontinuities in the primer coat, the second layer of CPC primer coat was applied and allowed to dry for 30 min. Later, sealant was applied on the primer coated steel surface and allowed to cure for a minimum of 6 h (as per manufacturer's guideline). The average final coating thickness was measured using a coating thickness gauge (Elcometer 456). It was ensured that the coating thickness is more than the minimum recommended coating thickness of 175  $\mu\text{m}$  [44]. In addition, moisture absorption test was conducted on 10 CPC coated steels. The following test procedure was followed: Uncoated steels were weighed to the precision of 0.0001 gm (W1). Then, CPC coating was applied on the surfaces of the steel. Then, the CPC coated steels were weighed to the precision of 0.0001 gm (W2). After that, Each coated steel was immersed in concrete simulated pore solution for 24 h. Later, these coated steels were removed from the solution and were wiped using cotton cloth to surface dry condition; and weighed to the precision of 0.0001 gm (W3). The difference in the mass (W3-W2) is the moisture absorbed by the coating material. The average absorbed moisture  $[(W3 - W2)/(W2 - W1) * 100]$  after 24 h immersion of CPC coated steel was found to be [mean:25, standard deviation: 1.33] % by weight of coating material.

Fig. 3 shows the photograph and schematic of macrocell specimens (200  $\times$  75  $\times$  75 mm in size) with one anodic rebar at the top and two cathodic rebars at the bottom, similar to the ASTM G109 (2013) specimen. The anode-to-cathode ratio of the test specimens was 0.5, as in ASTM G109 specimen. The AR steel surface is expected to have the mill scale and/or mild rust layer on the steel surfaces; whereas, SB steel surface is expected to be free from rust, dust, or any other foreign elements. AR and SB steel rebars of 10 mm diameter were cut to 200 mm length and were used as anodic and cathodic rebars. For the specimens with uncoated steel rebars, two thin layers of the epoxy coating were applied on the 25 mm long region at both ends of the rebars; and allowed to cure for two days. This region was further covered with a heat-shrink tube to avoid the entry of oxygen and moisture (see Fig. 3). For the specimens with coated steel rebars, Later, as it was done on uncoated steel rebars, the 25 mm long region at both ends of the

CPC coated steel rebars were covered with two thin layers of epoxy coats and a heat-shrink tube.

After positioning the prepared rebars in the mould, the mortar was placed in the mould to cast the macrocell specimen. In this study, the mortar was used (instead of concrete) because  $Cl_{th}$  is a steel-concrete interface (SCI) property, and it depends on the local characteristics (or microclimate) of the SCI. The microclimate at the SCI can change due to many factors, including the presence of aggregates [45]. However, the influence of the presence of inert aggregates on  $Cl_{th}$  is due to the indirect effect of the change in the microclimate of SCI. To avoid nonuniformities in the physical microclimate at the SCI, mortar was used to prepare the macrocell specimens. Also, the use of mortar can help to reduce the test duration and the size of the specimens. Many researchers have used mortar to quantify the  $Cl_{th}$  of various steel-cementitious systems [46–48]. Therefore, mortar with cement: sand: w/b of 1: 2.75: 0.5 was used to prepare the macrocell specimens. The Ordinary Portland Cement (53 Grade) with the requirements confirming with IS:12269 (2008) was used to prepare the mortar for the casting of macrocell specimens. Table 4 shows the chemical composition and physical properties of OPC used in this study. The Grade II and Grade III silica sand as per IS:383 (1970) was used in equal proportion by mass [49]. Distilled water was used to prepare all the macrocell specimens.

### 3.3.2. Exposure and electrochemical measurements

Macrocell specimens were cast and cured in the mould for one day; then, moist-cured for another 27 days. Then, the specimens were kept in an environment with a relative humidity of  $65 \pm 5\%$  and  $27 \pm 5^\circ\text{C}$  for the remaining exposure/testing period. Electrical connections using a 100  $\Omega$  resistor were made between the anode and cathodes. Silicone sealant was applied on the inclined side faces of the reservoir to enable one-dimensional chloride transport through mortar cover towards the embedded steel rebar. To accelerate the chloride transport, cyclic 2 days wet followed by 5 days dry regime using 15% sodium chloride solution was adopted. At the end of each wet period, the potential differences between the top and the bottom rebars were recorded across the 100  $\Omega$  resistor. These potential differences and Ohm's Law were used to calculate the macrocell corrosion rates every week. Then, the total corrosion was calculated using the trapezoidal rule. As per ASTM G109, when the total corrosion was reached to 150 Coulombs (C), the specimens were defined to have depassivated [50]. The chloride concentration at the steel surface at this instant was considered as  $Cl_{th}$ . Hence, when the total corrosion reached 150 C, the macrocell specimens were autopsied and the powder from the mortar near to the upper face of the top rebar was collected. Chloride concentrations of these powdered samples were determined using the guidelines given in SHRP-S-330 (1993) and defined as the  $Cl_{th}$  of the specimen [42].

### 3.4. Estimation of corrosion initiation time ( $t_i$ )

Service life assessment models, such as DuraCrete, Life-365<sup>TM</sup>, STADIUM<sup>®</sup>, are commercially available to estimate the corrosion initiation time of RC structures. A open source software (Life 365<sup>TM</sup>) developed by ACI Committee 365 was used for the estimation of corrosion initiation time/service life [43]. Life-365<sup>TM</sup> was chosen for this study because it considers  $C_{max}$ ,  $D_{ci}$ ,  $Cl_{th}$ , and  $m$  as input parameters to estimate the service life. It also allows the user to provide the coefficient of variation for each input variable. Also, probabilistic responses were obtained for the corrosion initiation time ( $t_i$ ).

**Table 3**  
Test variables and number of specimens.

Surface condition	Coating condition	Number of specimens
As-received (AR)	wC	5
	woC	5
Sand-blasted (SB)	wC	5
	woC	5
Total number of specimens		20

wC – with coating.

woC – without coating.

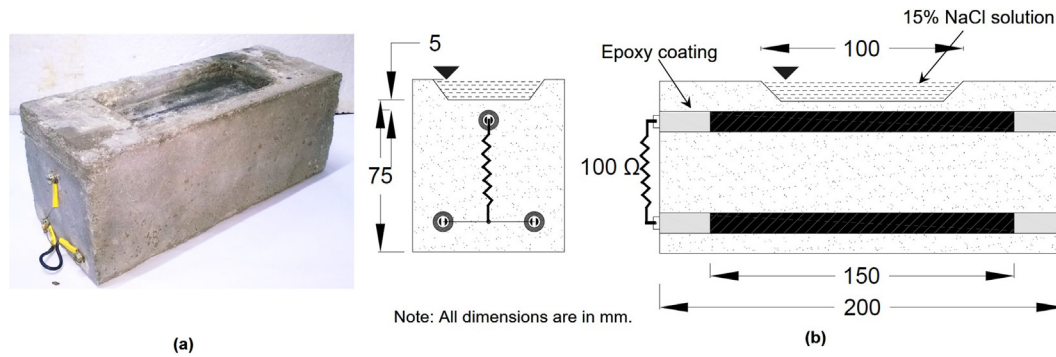


Fig. 3. Macrocell corrosion test specimen (similar to ASTM G109).

**Table 4**  
Chemical composition and physical properties of OPC used in this study.

Composition (%)						Physical properties		
Al <sub>2</sub> O <sub>3</sub>	Fe <sub>2</sub> O <sub>3</sub>	CaO	MgO	(Na <sub>2</sub> O)	LOI	Mean diameter (μm)	Specific surface area (m <sup>2</sup> /kg)	Specific gravity
5.54	4.71	61.7	1.06	0.2	2.27	15	330	3.15

#### 4. Results and discussions

The data on  $C_{max}$ ,  $D_{cl}$  and  $Cl_{th}$  were obtained from various experiments conducted on the concrete specimens obtained from the girder, pier, pile cap and pile of the 6-year old bridge and the steel specimens similar to those used in the bridge. The  $C_{max}$ ,  $D_{cl}$  and  $Cl_{th}$  were used as input parameters for the estimation of corrosion initiation time ( $t_i$ ) using Life-365™.

##### 4.1. Maximum chloride concentration at the concrete surface ( $C_{max}$ )

The average  $C_{max}$  of concrete specimens obtained from the girder, pier, pile cap, and pile were 1.16, 1.17, 1.29, and 2.94% by weight of binder (%bwob), respectively. The time required to build the  $C_{max}$  on the concrete surface ( $time_{C_{max}}$ ) depends of the porosity and the ion-exchange phenomenon at the near-surface concrete and the exposure conditions. Here, each element of the bridge is made of different concretes and exposed to different exposure conditions. For example, the girders and piers are exposed to airborne chlorides; whereas, the pile caps and piles are exposed to moist soil with chlorides. The average surface chloride concentrations ( $C_s$ ) at 6 years of exposure were found to be 0.1, 0.2, 0.9, and 2.6 %bwob for girder, pier, pile cap, and pile, respectively. Based on this, the rate of growth of  $C_s$  was determined assuming a linear increase. The  $time_{C_{max}}$  for the girder, pier, pile cap, and pile was estimated to be 65, 36, 10, and 6.5 years, respectively. These results are summarised in Table 5 and were used for estimating  $t_i$ .

##### 4.2. Chloride diffusion coefficient of concrete ( $D_{cl}$ )

Fig. 4(a)–(j) show the chloride profiles of the concrete specimens obtained from girders, piers, pile caps, and piles. Due to the significant variations in the leaching/chloride-ion exchange phe-

nomenon near the concrete surface, the chloride concentrations in the 5 mm thick layer near the concrete surface was not considered for determining the  $D_{cl}$  [35]. These chloride profiles and Fick's second law were used to determine the  $D_{cl}$  for each specimen. Note that these diffusion coefficients are determined at the age of 6 years. Hence,  $D_{cl}$  at 28 days were calculated by estimating the decay constant,  $m$ , from Eq. (3). As shown in Fig. 4(k), the average  $D_{cl}$  (at 28 days) after the construction of the girder, pier, pile cap, and pile were estimated to be 1.71, 1.9, 2.4, and  $2.7 \times 10^{-11}$  m<sup>2</sup>/s, respectively. Then, these diffusion coefficients were used for further assessment. The quality and uniformity in the construction practices (say, mixing, placement, compaction, curing, etc. of concrete) can significantly influence the variation in the transport properties of concrete. Higher the coefficients of variation (COV) of  $D_{cl}$ , the larger will be the uncertainty in the estimated  $t_i$ . In this study, the uncertainty in the  $t_i$  due to the  $D_{cl}$  of girder and pile caps were assessed using the COV of 36% and 6%, as exhibited by the three values of  $D_{cl}$  obtained. In the case of piers and piles, only two specimens could be obtained and tested for  $D_{cl}$ , for which the COV was assumed to be 25%.

##### 4.3. Chloride threshold of steel-coating-concrete interfaces ( $Cl_{th}$ )

Fig. 5 shows the total corrosion (in Coulombs) for AR-w/C, SB-w/C, AR-w/C, and SB-w/C specimens (with two cases in each graph). In this study, corrosion is defined to initiate when the total corrosion reached 150 C [50]. As shown in Fig. 5(a), the AR-w/C and SB-w/C specimens exhibited corrosion initiation at about 50 and 70 days of cyclic exposure, respectively. This delay in the onset of corrosion for SB-w/C specimens can be attributed to the formation of a uniformly thick and dense passive layer that is well-adhered to the SB steel surface with high surface energy [51]. On the other hand, the passive layer on AR steel surface may not exhibit uniform

**Table 5**  
Chloride transport properties of concrete for different structural elements.

Structural element	$m$	$D_{cl}$ (m <sup>2</sup> /s)	$C_s$ (% bwob)	$C_{max}$ (% bwob)	$time_{C_{max}}$ (years)
Girder (M60)	0.38	$1.71 \times 10^{-11}$	0.1	1.16	65
Pier (M45)	0.42	$1.90 \times 10^{-11}$	0.2	1.17	36
Pile cap (M35)	0.45	$2.37 \times 10^{-11}$	0.9	1.29	10
Pile (M35)	0.45	$2.69 \times 10^{-11}$	2.6	2.94	6.5

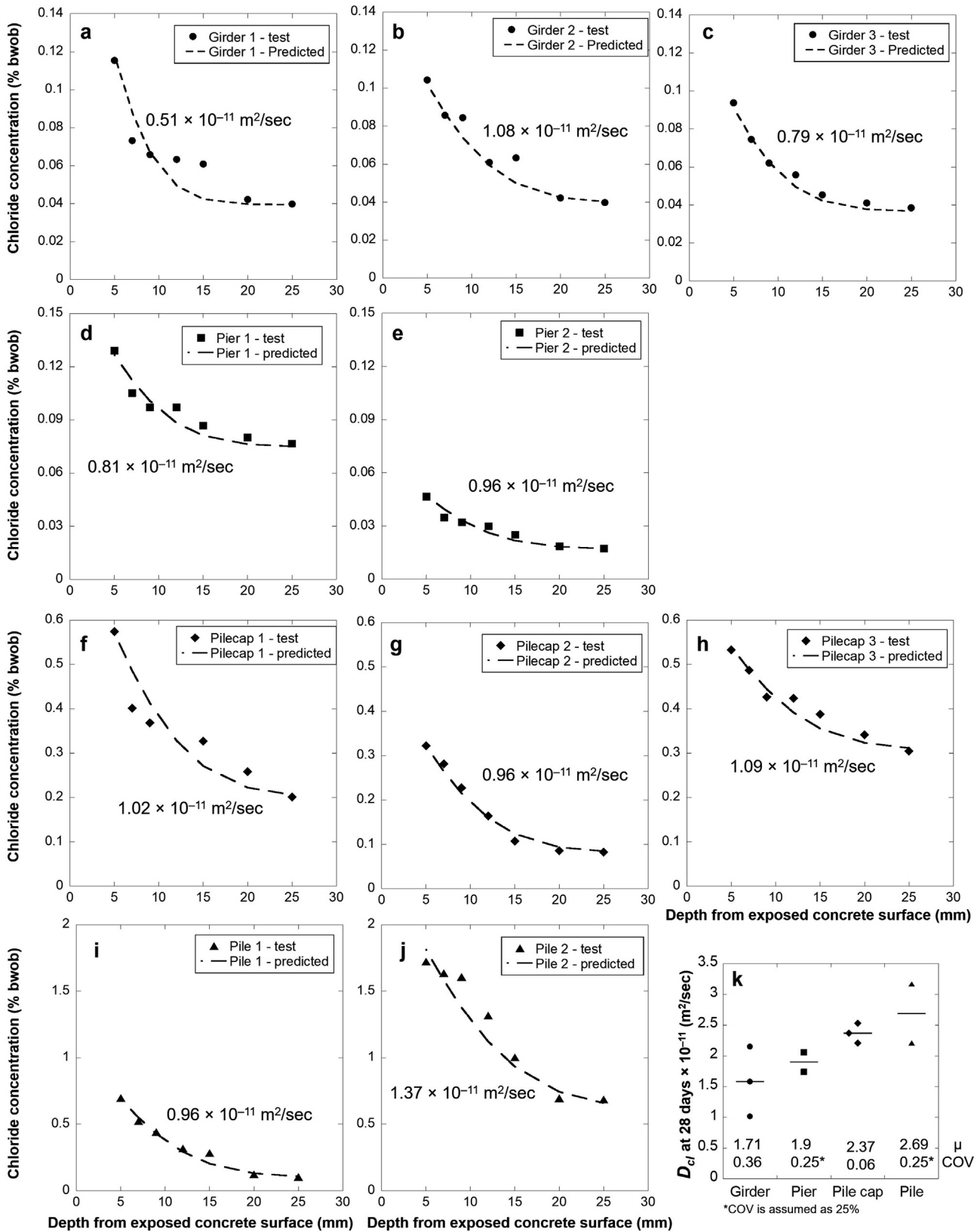


Fig. 4. Chloride profiles and diffusion coefficients for various concrete specimens cored from the bridge elements.

thickness and may be porous due to the presence of rust and dust particles on the steel surface [52].

Fig. 5 (b) shows that the AR-woC and AR-wC specimens exhibited corrosion initiation at the same time. The effect of the coating

is not realized due to the inadequacy in the preparation of steel surface before the application of CPC coating. For example, two AR-wC specimens exhibited corrosion along with all the AR-woC specimens at about 60 days of cyclic exposure. Authors observed

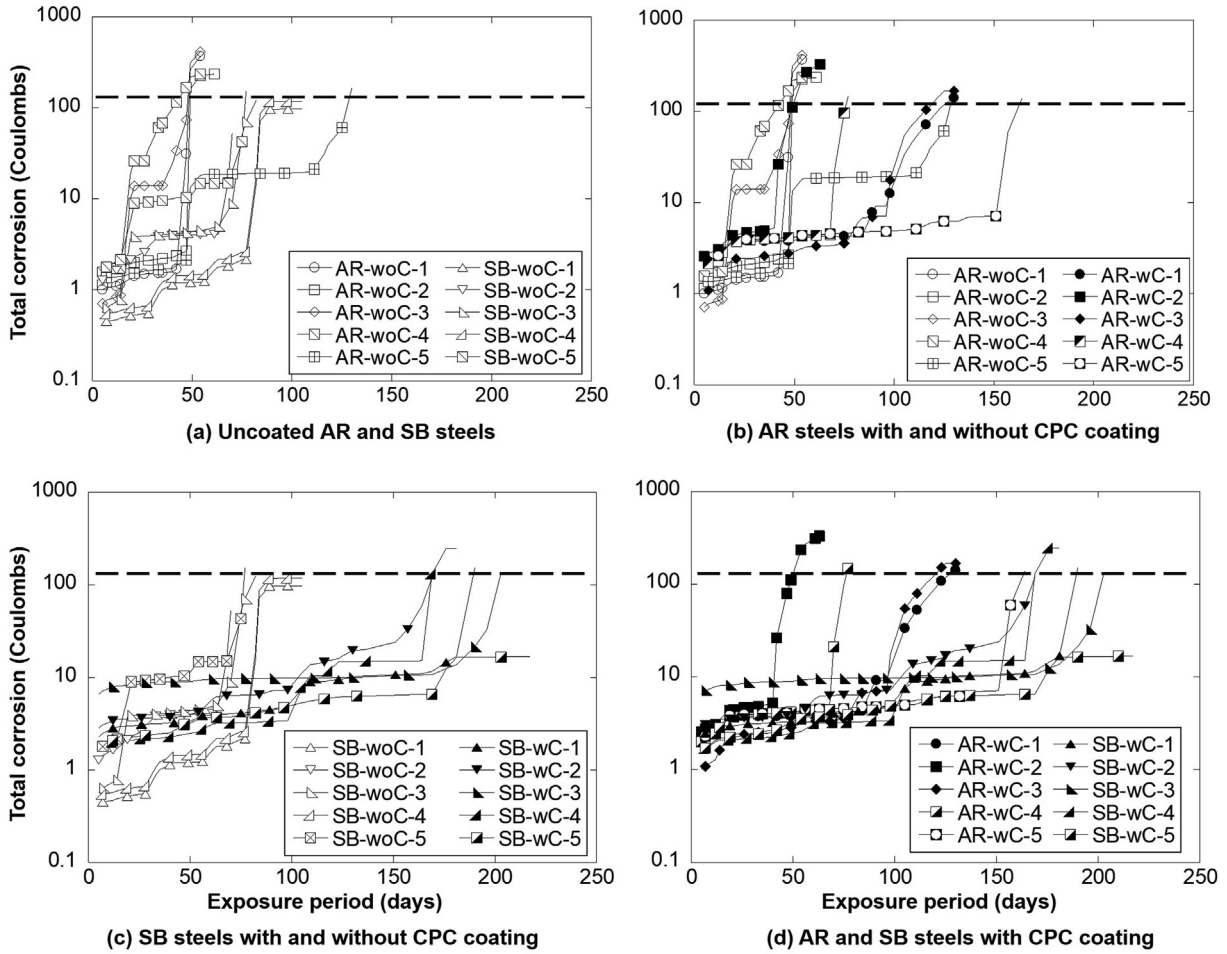


Fig. 5. Total corrosion measurements of various macrocell specimens.

that the rust on the steel surface offered traction during the application of the coating. As a result, the intermittent microcracks were observed between the steel and CPC coating (see Fig. 6(a)). It was experimentally found that the CPC coating can absorb about [mean: 25, standard deviation: 1.33]% moisture by weight of the coating material. If the coating does not adhere to the steel surface, it may not be able to provide the stable passive film to the steel surface, and chlorides with moisture can penetrate through the coating and lead to localized and premature corrosion. In addition,

the rust layer might absorb the moisture and maintain a corrosive environment between the steel and coating. This moist rust layer can provide a low resistance path for ionic transfer and lead to premature corrosion, even with low chloride levels. It can be concluded that the CPC coating exhibits no improvement in corrosion resistance when applied on the AR surface (see Fig. 7).

Fig. 5(c) shows that the SB-woC and SB-wC specimens exhibited corrosion initiation at about 70 and 200 days of exposure, respectively. Therefore, there is a significant improvement in corrosion

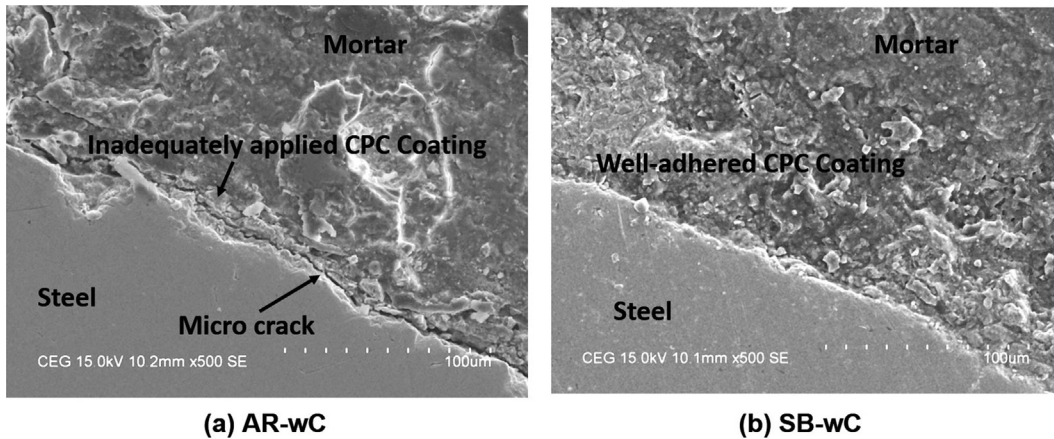


Fig. 6. SE images of the steel-coating-mortar interface.

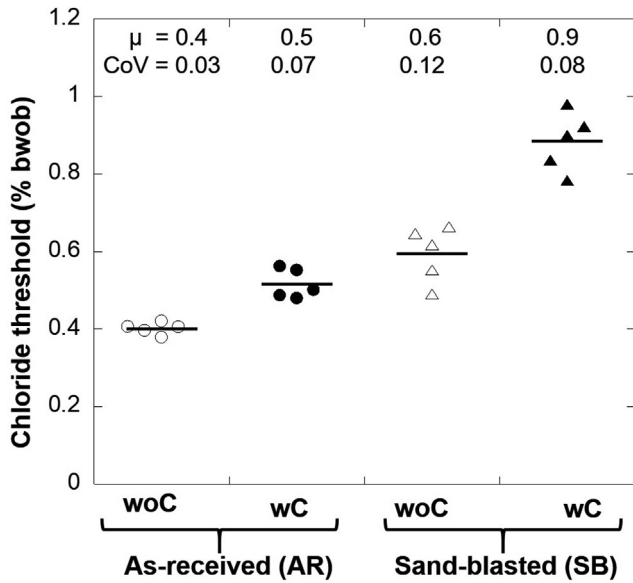


Fig. 7. Chloride thresholds of uncoated and CPC coated steels.

resistance when the coating is applied to clean/sand-blasted steel surface. This is mainly due to the physical barrier provided by the coating, which is well-adhered to the steel surface [see Fig. 6 (b)]. Many site personnel have the wrong perception that the CPC coating can perform well even without sandblasting or cleaning of steel surface. To address this, Fig. 5(d) provides evidence that the AR specimens with CPC coating exhibited corrosion initiation between 50 and 100 days of exposure. This large scatter could also be attributed to the variation in the quality of coating when applied on the as-received steel surface. On the other hand, the SB-wC specimens exhibited corrosion only after 200 days of cyclic exposure - indicating the highest corrosion resistance among the cases studied. Table 6 summarizes the time to corrosion initiation for AR-woC, AR-wC, SB-woC, SB-wC was found to be 70, 110, 80, and 200 days, respectively. The system with sandblasting and coating (SB-wC) could significantly delay the corrosion initiation process

Table 6  
Average exposure time required for initiation of corrosion in various cases.

Specimen type	Corrosion initiation time (days) [mean, standard deviation]
AR-woC	~LN [70, 30]
AR-wC	~LN [110, 45]
SB-woC	~LN [80, 30]
SB-wC	~LN [200, 30]

to approximately twice the duration observed in the case of AR-wC. This is because when CPC coating is applied on the SB surface, it can provide (i) high resistance to chloride penetration due to better continuity of the CPC coating, ii) reduced ionic transfer, iii) good adherence between the steel and CPC coating and iv) limited availability of oxygen to the steel substrate.

Upon corrosion initiation, the specimens were autopsied. The powdered mortar samples were collected from the mortar adjacent to the top rebar. The chloride concentrations in the collected powder were determined using the guidelines given in SHRP-330 (1993) and defined as  $Cl_{th}$ . Fig. 7 shows that the statistical distributions of  $Cl_{th}$  [expressed as ~LN( $\mu$ , COV) %bwob] of AR-woC, AR-wC, SB-woC, and SB-wC specimens were ~LN(0.4, 0.03), ~LN(0.5, 0.07), ~LN(0.6, 0.12), ~LN(0.9, 0.08) %bwob, respectively. The average  $Cl_{th}$  of SB-wC specimens was found to be significantly higher (i.e., 0.9% bwob) than the other cases. This indicates that the full potential of CPC coating can be exploited only when it is applied on SB steel surface.

The corroded steel surfaces of all the specimens were visually observed and photographs were taken. Fig. 8 shows sketches of various types of steel specimens showing the regions with corrosion and/or debonded coating. The dark-shaded regions in Fig. 8 (a) shows that the large surface area of rebars in AR-woC specimens were corroded; whereas, for SB-woC type specimen, corrosion was limited to a smaller surface area [see Fig. 8 (c)]. This is evidence of the formation of a stable and uniform passive layer on SB-woC steel specimens. Fig. 8 (b) shows the corroded surface of AR-wC specimens; where a larger area of rebar surfaces was found to be corroded, and a significant coating was debonded from the steel surface - indicating the under-film corrosion. This is because of the low resistance path offered by the possible moist

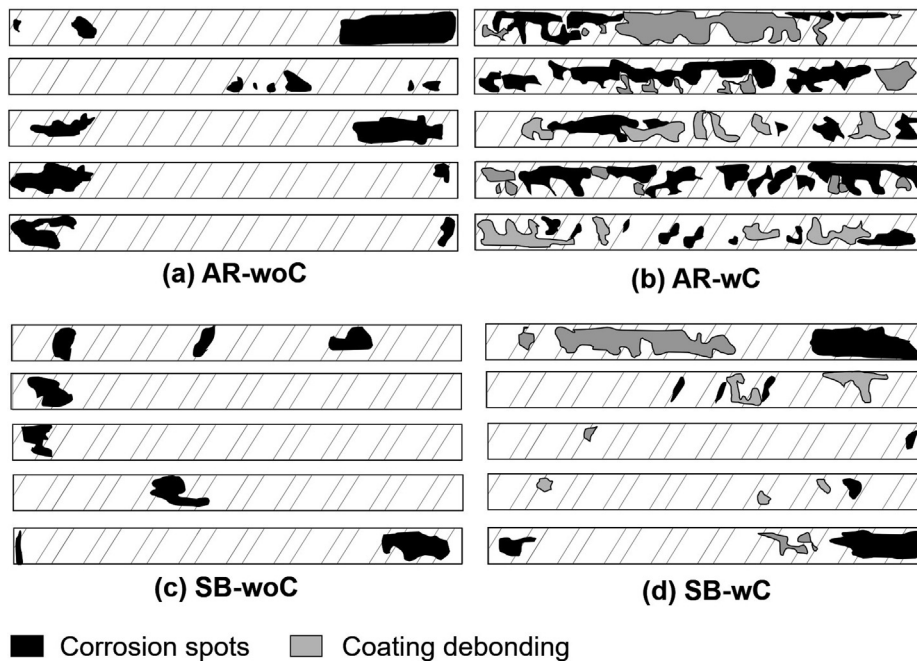


Fig. 8. Schematic of corroded surfaces of various rebars at the end of the test.

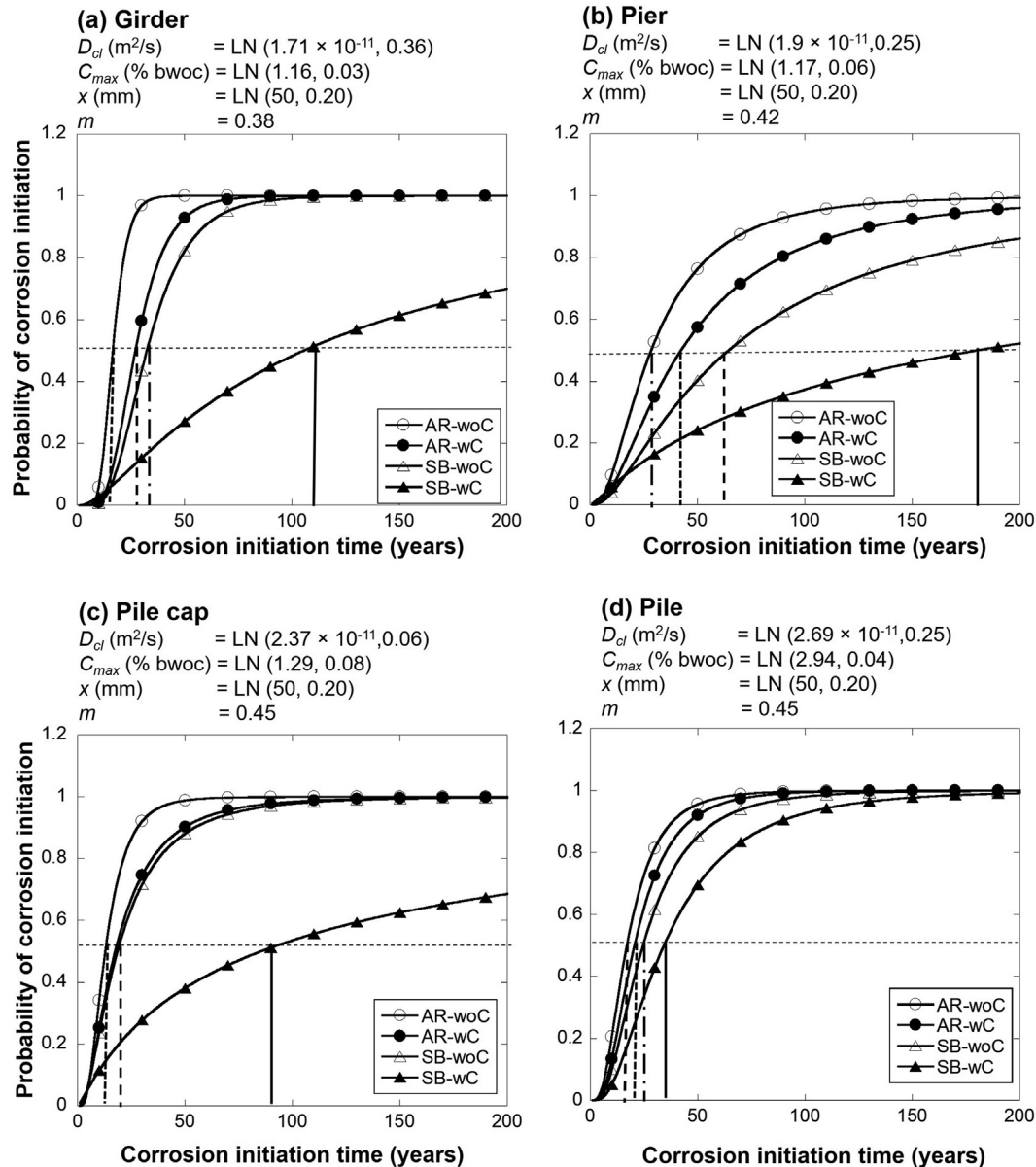


Fig. 9. CDF of corrosion initiation time for a) girder, b) pier, c) pile cap, and d) pile.

rust layer between the steel substrate and CPC coating (see the typical long and continuous microcrack in Fig. 6 (a)).

However, as shown in Fig. 8 (d), when sandblasting is done prior to the application of CPC coating, limited corrosion was observed. This indicates that the CPC coating was continuous and well-adhered to the sand-blasted steel surface – resulting in limited entry of chlorides. Also, once the corrosion was initiated, the ionic conduction was reduced due to the limited steel surface available as cathode – resulting in minimal under film/crevice corrosion. Therefore, it is suggested to use CPC coated rebar only when the steel surface is clean.

#### 4.4. Estimation of corrosion initiation time ( $t_i$ )

In this study, service life is defined as the time to corrosion initiation ( $t_i$ ). Life-365™ (2016) was used to estimate the  $t_i$  of the girder, pier, pile cap, and pile elements of the bridge under study. Fig. 9(a)–(d) shows the Cumulative Distribution Function (CDF) of  $t_i$  for the girder, pier, pile cap, and pile elements, respectively. For this, the probability of 50% of corrosion initiation was consid-

ered to be the end of service life. The input parameters, such as  $D_{cl}$ ,  $C_{max}$ , concrete cover ( $x$ ), and ‘ $m$ ’ for each case are given adjacent to the respective CDFs. In each case,  $t_i$  for AR-wC specimens was found to be at least 50% less than SB-wC specimens. The estimated  $t_i$  for the best case (SB-wC) of pile caps and piles was found 90 and 40 years, respectively; which is significantly shorter than the original design life of 120 years. It should be noted that the pile cap and pile elements are underground; where availability of oxygen is limited and therefore, the corrosion rate of rebars could be less [53]. However, sufficient oxygen can be available for 1 to 2 m below the ground level and the corrosion rate within this region for pile cap and pile could be high when sufficient chlorides are available – leading to premature corrosion of these elements [53].

## 5. Remedial measures

A large number of structures with poor quality CPC coating are constructed. Unfortunately, many more are being constructed, especially in the coastal zone with high levels of chlorides [47]. If the application of CPC coating is continued to be applied on rusted

rebar, soon many structures will face premature corrosion and the cost of repair will be significant. Therefore, site personnel should be insisted to sand-blast the rebars prior to the application of CPC coatings or order only the necessary and small quantities of steel (with minimal storage requirements), as being practiced in many parts of the world. In this way, they do not get exposed for long-term and experience corrosion by the time of application of the coating. For new structures, if such quality practices cannot be assured then it is strongly recommended to avoid the on-site application of CPC coatings. For the existing structures, cathodic prevention systems using galvanic anodes could be installed to delay the onset of corrosion. A small investment of about 3% of the total project cost before the onset of corrosion can significantly delay the initiation of corrosion [10]. Once, corrosion starts, it is more difficult and expensive to install an efficient cathodic protection system – hence, cathodic prevention is recommended.

## 6. Summary and conclusions

Recently, many infrastructure systems (railways/highways) have been constructed using Cement-Polymer-Composite (CPC) coated steel rebars. Many of them are constructed with poor quality coatings. One such bridge was considered for this study; where CPC coating material was applied on as-received steel rebar with a layer of rust (instead of the clean sand-blasted surface). In order to assess the quality of concrete used, cylindrical concrete specimens were extracted from the various elements on the bridge. Experiments were performed to determine surface chloride concentrations ( $C_s$ ), maximum surface chloride concentrations ( $C_{max}$ ), and diffusion coefficients ( $D_{cl}$ ). To quantify the differences in the chloride threshold ( $Cl_{th}$ ) of coated and uncoated as-received (AR) and sand-blasted (SB) steel specimens, macrocell corrosion tests were conducted on specimens with four steel surface and coating conditions. Then, Life-365™ was used to estimate the corrosion initiation time.

Experimental results show that the lack of cleaning/sandblasting prior to the application of CPC coating can lead to 50% reduction of the  $Cl_{th}$ . Visual inspection of corroded surfaces of steel specimens also indicated that when CPC coating was applied on the sand-blasted steel surface, the coating could adhere well to steel surface – resulting in higher resistance to ionic transfer and under-film corrosion. This was justified using the SEM images showing microcracks in the case of as-received specimens and well-adhered interfaces in the case of sand-blasted specimens. In addition, significant scatter was observed on the chloride diffusion coefficient of concrete used in the bridge. Combining the effects of chloride threshold and chloride diffusion coefficient, the probabilistic corrosion initiation time ( $t_i$ ) was obtained; it was found that the structures with inadequately coated steel reinforcement might exhibit about 50% less average service life than expected. Therefore, surface preparation (rust removal) prior to the application of CPC coating is an important step to achieve the desired service life of RC structures.

## Declaration of Competing Interest

The authors declare that they have no known competing financial interests or personal relationships that could have appeared to influence the work reported in this paper.

## Acknowledgements

The authors acknowledge the financial support (Project No. EMR/2016/003196) received from the Department of Science and Technology, and other financial support from the MHRD (Ministry

of Human Resource Development) of the Government of India. Authors are grateful to the Larsen & Toubro Construction for providing materials and field specimens. The authors also acknowledge assistance from the laboratory staff and students in the Construction Materials Research Laboratory (CMRL) at the Indian Institute of Technology Madras, Chennai, India.

## References

- [1] B. Biaz, X.R. Nóvoa, C. Pérez, A. Pintos, EIS study of epoxy resin applied on carbon steel using double-cylinder electrolyte cell, *Prog. Org. Coat.* 124 (2018) 275–285, <https://doi.org/10.1016/j.porgcoat.2018.02.002>.
- [2] E.V. Cortés, *Corrosion Performance of Epoxy-Coated Reinforcement in Aggressive Environments*, The University of Texas at Austin (1998).
- [3] S. Kessler, M. Zintel, C. Gehlen, Defects in epoxy-coated reinforcement and their impact on the service life of a concrete structure A study of critical chloride content and macro-cell corrosion, *Struct. Concr.* (2015) 398–405, <https://doi.org/10.1002/suco.201400085>.
- [4] A.N. Ababneh, M.A. Sheban, M.A. Abu-Dalo, Effectiveness of benzotriazole as corrosion protection material for steel reinforcement in concrete, *J. Mater. Civ. Eng.* 24 (2012) 141–151, [https://doi.org/10.1061/\(ASCE\)MT.1943-5533.0000374](https://doi.org/10.1061/(ASCE)MT.1943-5533.0000374).
- [5] M. Criado, I. Sobrados, J.M. Bastidas, J. Sanz, Corrosion behaviour of coated steel rebars in carbonated and chloride-contaminated alkali-activated fly ash mortar, *Prog. Org. Coat.* 99 (2016) 11–22, <https://doi.org/10.1016/j.porgcoat.2016.04.040>.
- [6] F. Tang, G. Chen, J.S. Volz, R.K. Brow, M.L. Koenigstein, Cement-modified enamel coating for enhanced corrosion resistance of steel reinforcing bars, *Cem. Concr. Compos.* 35 (2013) 171–180, <https://doi.org/10.1016/j.cemconcomp.2012.08.009>.
- [7] R. Vedalakshmi, K. Kumar, V. Raju, N.S. Rengaswamy, Effect of prior damage on the performance of cement-based coatings on rebar: Macrocell corrosion studies, *Cem. Concr. Compos.* 22 (2000) 417–421, [https://doi.org/10.1016/S0958-9465\(00\)00041-X](https://doi.org/10.1016/S0958-9465(00)00041-X).
- [8] P. Venkatesan, N. Palaniswamy, K. Rajagopal, Corrosion performance of coated reinforcing bars embedded in concrete and exposed to natural marine environment, *Prog. Org. Coat.* 56 (2006) 8–12, <https://doi.org/10.1016/j.porgcoat.2006.01.011>.
- [9] G. Koch, J. Varney, N. Thompson, O. Moghissi, M. Gould, J. Payer, *International Measures of Prevention, Application, and Economics of Corrosion Technologies Study*, NACE International (2016) 1–30. <http://impact.nace.org/documents/Nace-International-Report.pdf>.
- [10] A. Byrne, N. Holmes, B. Norton, State-of-the-art review of cathodic protection for reinforced concrete structures, *Mag. Concr. Res.* 68 (2016) 664–677, <https://doi.org/10.1680/jmacr.15.00083>.
- [11] J. Zemajitis, R.E. Weyers, M.M. Sprinkel, An evaluation of the performance of epoxy-coated reinforcing steel in concrete exposure specimens, *Final Contract Rep. by Virginia Transportation Research Council 147* (1998) p.
- [12] A. Griffith, H.M. Laylor, *Epoxy coated Final Report*, Security (1999).
- [13] R.E. Weyers, M. Ryan, D.W. Mokarem, Jerzy Zemajitis, Michael M. Sprinkel, John G. Dillard, *Field performance of epoxy-coated reinforcing steel in Virginia bridge decks*, *Environ. Eng. Blacksburg, Virginia* (1998).
- [14] F. Fanous, H. Wu, Performance of coated reinforcing bars in cracked bridge decks, *J. Bridge Eng.* 10 (2005) 255–261, [https://doi.org/10.1061/\(ASCE\)1084-0702\(2005\)10:3\(255\)](https://doi.org/10.1061/(ASCE)1084-0702(2005)10:3(255)).
- [15] B. Biegafiska, M. Zubielewicz, E. Qmiesz, Influence of barrier pigments on the performance of protective organic coatings, *Prog. Org. Coat.* 16 (1988) 219–229.
- [16] L. Guadagno, M. Raimondo, V. Vittoria, L. Vertuccio, C. Naddeo, S. Russo, B. De Vivo, P. Lamberti, *R. Soc. Chem. Adv.* (2014) 15474–15488, <https://doi.org/10.1039/c3ra48031c>.
- [17] X. Xue, J. Yang, W. Zhang, L. Jiang, J. Qu, L. Xu, H. Zhang, The study of an energy efficient cool white roof coating based on styrene acrylate copolymer and cement for waterproofing purpose – Part I: optical properties, estimated cooling effect and relevant properties after dirt and accelerated exposures, *Constr. Build Mater. J.* 98 (2015) 176–184, <https://doi.org/10.1016/j.conbuildmat.2015.08.045>.
- [18] S.B. Lyon, R. Bingham, D.J. Mills, Progress in Organic Coatings Advances in corrosion protection by organic coatings: what we know and what we would like to know, *Prog. Org. Coat.* 102 (2017) 2–7, <https://doi.org/10.1016/j.porgcoat.2016.04.030>.
- [19] X. Xue, J. Yang, W. Zhang, L. Jiang, J. Qu, L. Xu, H. Zhang, J. Song, R. Zhang, Y. Li, J. Qin, Z. Zhang, The study of an energy efficient cool white roof coating based on styrene acrylate copolymer and cement for waterproofing purpose – Part II : Mechanical and water impermeability properties, *Constr. Build Mater.* 96 (2015) 666–672, <https://doi.org/10.1016/j.conbuildmat.2015.08.033>.
- [20] J.E.O. Mayne, The mechanism of the protection of iron and steel by paint, *Anti Corrosion* (1973) 3–8.
- [21] R. Selvaraj, M. Selvaraj, S.V.K. Iyer, Studies on the evaluation of the performance of organic coatings used for the prevention of corrosion of steel rebars in concrete structures, *Prog. Org. Coat.* 64 (2009) 454–459, <https://doi.org/10.1016/j.porgcoat.2008.08.005>.

- [22] H.G. Wheat, G. Liu, Monitoring the corrosion behavior of coated reinforcement for concrete, *ECS Trans.* 3 (2007) 71–79.
- [23] F. Tang, Y. Bao, Y. Chen, Y. Tang, G. Chen, Impact and corrosion resistances of duplex epoxy/enamel coated plates, *Constr. Build. Mater.* 112 (2016) 7–18, <https://doi.org/10.1016/j.conbuildmat.2016.02.170>.
- [24] M.S.H.S. Mohammed, R.S. Raghavan, G.M.S. Knight, V. Murugesan, Macrocell corrosion studies of coated rebars, *Arab. J. Sci. Eng.* 39 (2014) 3535–3543, <https://doi.org/10.1007/s13369-014-1006-x>.
- [25] X.H. Wang, Y. Gao, Corrosion behavior of epoxy-coated reinforced bars in RC test specimens subjected to pre-exposure loading and wetting, *Constr. Build. Mater.* 119 (2016) 185–205, <https://doi.org/10.1016/j.conbuildmat.2016.05.066>.
- [26] D.G. Manning, Corrosion performance of epoxy-coated reinforcing steel: North American experience, *Constr. Build. Mater.* 10 (1996) 349–365.
- [27] D.D.N. Singh, R. Ghosh, Unexpected deterioration of fusion-bonded epoxy-coated rebars embedded in chloride-contaminated concrete environments, *Corrosion* 61 (2005) 815–829.
- [28] J. Marsh, J.D. Scantlebury, S.B. Lyon, The effect of surface/primer treatments on the performance of alkyd coated steel, *Corros. Sci.* 43 (2001) 829–852, [https://doi.org/10.1016/S0010-938X\(00\)00070-6](https://doi.org/10.1016/S0010-938X(00)00070-6).
- [29] X. Pei, M. Noël, A. Fam, M. Green, Development length of steel reinforcement with corrosion protection cementitious coatings, *Cem. Concr. Compos.* 60 (2015) 34–43, <https://doi.org/10.1016/j.cemconcomp.2015.04.003>.
- [30] X. Pei, M. Noël, M. Green, A. Fam, G. Shier, Cementitious coatings for improved corrosion resistance of steel reinforcement, *Surf. Coat. Technol.* 315 (2017) 188–195, <https://doi.org/10.1016/j.surfcoat.2017.02.036>.
- [31] S. Jorge, D. Dias-da-Costa, E.N.B.S. Júlio, Influence of anti-corrosive coatings on the bond of steel rebars to repair mortars, *Eng. Struct.* 36 (2012) 372–378, <https://doi.org/10.1016/j.engstruct.2011.12.028>.
- [32] K. Wang, Z. Liu, Z. Wang, W. Yang, Study on polymer modified cement-based coating with healing effect on rusty carbon steel, *Int. J. Corrosion* (2014), <https://doi.org/10.1155/2014/628191>.
- [33] R.R. Hussain, Effect of moisture variation on oxygen consumption rate of corroding steel in chloride contaminated concrete, *Cem. Concr. Compos.* 33 (2011) 154–161, <https://doi.org/10.1016/j.cemconcomp.2010.09.014>.
- [34] M. Shakouri, D. Trejo, A study of the factors affecting the surface chloride maximum phenomenon in submerged concrete samples, *Cem. Concr. Compos.* 94 (2018) 181–190.
- [35] M. Shakouri, D. Trejo, A time-variant model of surface chloride build-up for improved service life predictions, *Cem. Concr. Compos.* 84 (2017).
- [36] H.-W. Song, C.-H. Lee, K.Y. Ann, Factors influencing chloride transport in concrete structures exposed to marine environments, *Cem. Concr. Compos.* 30 (2008) 113–121, <https://doi.org/10.1016/j.cemconcomp.2007.09.005>.
- [37] K.Y. Ann, J.H. Ahn, J.S. Ryou, The importance of chloride content at the concrete surface in assessing the time to corrosion of steel in concrete structures, *Constr. Build. Mater.* 23 (2009) 239–245, <https://doi.org/10.1016/j.conbuildmat.2007.12.014>.
- [38] J. Němeček, J. Krus, T. Koudelka, T. Krejčí, Simulation of chloride migration in reinforced concrete, *Appl. Math. Comput.* 319 (2018) 575–585, <https://doi.org/10.1016/j.amc.2017.07.029>.
- [39] D. Nuralinah, Laboratory test and numerical analysis of chloride ingress into concrete subjected into airborne salt (Ph.D. thesis), Nagaoka Univ. Technol. Nagaoka, Niigata, 2012.
- [40] NT Build 492, Concrete, mortar and cement-based repair materials: Chloride migration coefficient from non-steady-state migration experiments, FINLAND, 1999.
- [41] ASTM C1556 – 11a, 1556, Standard Test Method for Determining the Apparent Chloride Diffusion Coefficient of Cementitious Mixtures by Bulk Diffusion, Annual Book of ASTM Standards, vol. 4.02, 2015, doi:10.1520/C1556-11A.2.
- [42] SHRP-S-330, Standard Test Method for Chloride Content in Concrete Using the Specific Ion Probe, (1993) 1–118
- [43] E.C. Bentz, Probabilistic modeling of service life for structures subjected to chlorides, *ACI Mater. J.* (2003) 391–397.
- [44] ASTM A775/A775M – 17, Standard Specification for Epoxy-Coated Steel Reinforcing Bars 1, 2017, doi:10.1520/A0775.
- [45] U.M. Angst, M.R. Geiker, A. Michel, C. Gehlen, H. Wong, O.B. Isgor, B. Elsener, C. M. Hansson, R. François, K. Hornbostel, R. Polder, M.C. Alonso, M. Sanchez, M.J. Correia, M. Criado, A. Sagüés, N. Buenfeld, The steel–concrete interface, *Mater. Struct.* 50 (2017) 143, <https://doi.org/10.1617/s11527-017-1010-1>.
- [46] J. Karuppanasamy, R.G. Pillai, A short-term test method to determine the chloride threshold of steel – cementitious systems with corrosion inhibiting admixtures, *Mater. Struct.* 50 (2017) 1–17, <https://doi.org/10.1617/s11527-017-1071-1>.
- [47] J. Karuppanasamy, R.G. Pillai, Statistical distributions for the corrosion rates of conventional and prestressing steel reinforcement embedded in chloride contaminated mortar, *Corrosion J.* 73 (2017) 1119–1131.
- [48] S. Rengaraju, L. Neelakantan, R.G. Pillai, Investigation on the polarization resistance of steel embedded in highly resistive cementitious systems - An attempt and challenges, *Electrochim. Acta* 308 (2019) 131–141, <https://doi.org/10.1016/j.electacta.2019.03.200>.
- [49] IS:383, Specification for coarse and fine aggregates from natural sources for concrete, Bureau of Indian Standards, 1970.
- [50] ASTM G109 – 07, Standard Test Method for Determining the Effects of Chemical Admixtures on the Corrosion of Embedded Steel Reinforcement in Concrete Exposed to Chloride Environments, 2013.
- [51] L. Ding, H. Torbati-sarrafi, A. Poursaeed, The influence of the sandblasting as a surface mechanical attrition treatment on the electrochemical behavior of carbon steel in different pH solutions, *Surf. Coat. Technol.* 352 (2018) 112–119, <https://doi.org/10.1016/j.surfcoat.2018.08.013>.
- [52] L. Ding, A. Poursaeed, The impact of sandblasting as a surface modification method on the corrosion behavior of steels in simulated concrete pore solution, *Constr. Build. Mater.* 157 (2017) 591–599, <https://doi.org/10.1016/j.conbuildmat.2017.09.140>.
- [53] R.M. Azoor, R.N. Deo, N. Birbilis, J. Kodikara, On the optimum soil moisture for underground corrosion in different soil types, *Corros. Sci.* (2019), <https://doi.org/10.1016/j.corsci.2019.108116>.